Forced response of a vertical rotor with tilting pad bearings

Erik Synnegård[1]*, Rolf Gustavsson[2], Jan-Olov Aidanpää[1]

ISROMAC 2016

International Symposium on Transport Phenomena and Dynamics of Rotating Machinery

Hawaii, Honolulu

April 10-15, 2016

Abstract

This paper evaluates how tilting pad bearings can affect the forced response of a vertical rotor. The stiffness and damping for a tilting pad bearing is dependent on the position in the bearing (load on pad or load between pad) and the magnitude of the load. In a vertical machine the position of the shaft in the bearing will change for each time-step and produce a periodic stiffness and damping. This periodic stiffness has shown to produce higher frequency components depending on the number of pads. For the four pad bearing considered in this paper these frequency components are 3Ω and 5Ω in the stationary coordinate system. The aim of this study is to evaluate if the periodic coefficients in the bearing could excite the system and cause resonance problems. It is found that for high loads the system can be excited due to the bearing dynamics at $\Omega/\omega_n = 0.33$ and $\Omega/\omega_n = 0.2$. However at low loads this effect is negligible.

Keywords

Vertical Rotor — Tilting Pad Bearing

[1] *Department of Engineering Sciences and Mathematics, Luleå University of Technology, Luleå, Sweden*
[2] *Vattenfall Research and Development, Älvkarleby, Sweden*
***Corresponding author**: erik.synnegard@ltu.se

INTRODUCTION

Tilting pad journal bearings (TPJB) have been used in rotating machines since the early 1900's and describing the bearing coefficients dynamically has been studied extensively in the last 60 years. TPJB's are commonly used as supports in hydropower machines and offshore pumps because of their good stability. Since hydropower machines are orientated vertically there exists no stationary operating point in the bearing due to the dead weight of the rotor. Hence, in hydropower machines and vertical pumps, the bearing coefficients need to be described dynamically at each time step. In 1964 Lund [1] published a paper where he introduced the pad assembly method and the Reynolds equation solution to solve the bearing coefficients. Over the last 50 years bearing theory has evolved, Timothy et.al [2] published a review of tilting pad bearing theory. Current state of the art now include inertia effects, pad motions, thermal and mechanical deformations. However, modelling the bearing coefficients dynamically for vertical machines using e.g. Reynolds equations have been performed earlier by M.Cha et.al[3] and White et.al[4]. Moreover, modelling the bearing dynamically using Reynolds takes time and if rotordynamical studies are to be performed, acceptable simplified methods are preferred. For example in rotordynamics there is a need to simulate a lot of periods to reach steady state and evaluate large parameter intervals. For these cases solving Reynolds equation at each time-step would take to long time, while with the bearing model used in this paper 100 periods for this 16 DOF model takes around 4 hours on a standard laptop. Nässelqvist et.al [5] proposed a method to describe the bearing coefficients dynamically as function of eccentricity and load angle. In vertical machines the bearing coefficients are dependent on shaft position and eccentricity in the bearing, this will introduce periodic coefficients, which depends on the number of pads. Earlier studies of a vertical Jeffcott rotor with two 4-pad bearings shows that higher frequency components at 3Ω and 5Ω exist in the unbalance response, see Figure 1. In that case the shaft can be consider rigid since the aim of the study was the bearing modeling. In this paper the effects of these higher frequency components are studied where the aim is to analyse if these higher frequency components could excite the machine and cause resonance problems. The rotor in this study is similar to the one studied earlier but with a more slender shaft. In addition, experiments are also planned to see if this also can be observed experimentally.

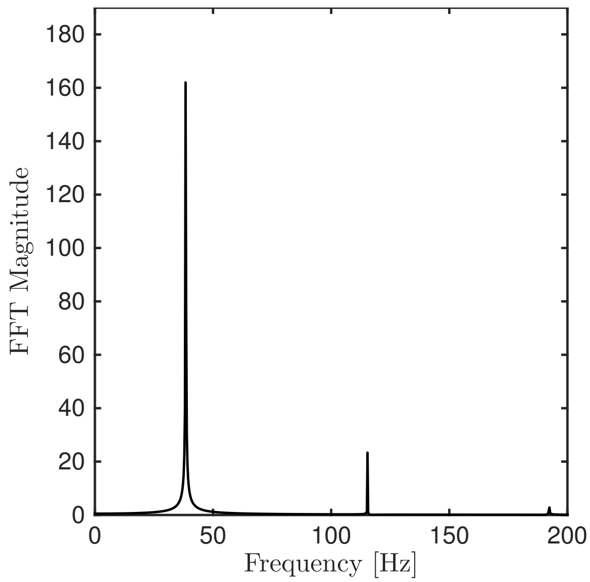

Figure 1. Fourier transform of the bearing load from earlier simulations.

1. METHODS

1.1 Rotor description

The rotor used for simulations is a vertically orientated Jeffcott rotor, see Figure 2. The rotor is modelled using 3 nodes (12 DOF's) for the shaft. At node 1 and node 3 tilting pad bearings supports the rotor, which is connected to ground through bearing brackets. Parameters for the rotor is, shaft diameter d_1 = 20.00 mm, disk diameter D = 168 mm and length L = 500 mm between the bearing centres. Due to limitations in bearing design the shaft diameter at the bearing locations are set to d_2 = 49.84. In Table 1 the rotor and bearing properties are presented.

1.2 Bearing model

For a vertical machine with tilting pad bearings the stiffness and damping varies periodically depending on the number of pads in the bearing. In Figure 3 a sketch of a 4-pad tilting pad bearing is shown. Using a commercial bearing software [6] the bearing data can be calculated as function of load angle for a fixed load in the local coordinate system (ξ,η) and this is presented in Figure 4. Here 0° represent load on pad (LOP) and ±45° represent load between pad (LBP). Also in Figure 4 the stiffness as function of eccentricity is presented, it can be seen that the difference between load on pad and load between pad increases for larger eccentricities. Note, only the bearing stiffness is presented in Figure 4 but the same behaviour is observed for the damping. The bearing coefficients are calculated using Nässelqvist's [5] method, where a polynomial fit is made to describe the stiffness and damping for LOP and LBP as function of eccentricity ϵ. This polynom is then used to describe the bearing coefficients for a given load angle and eccentricity according to equation 1 and 2.

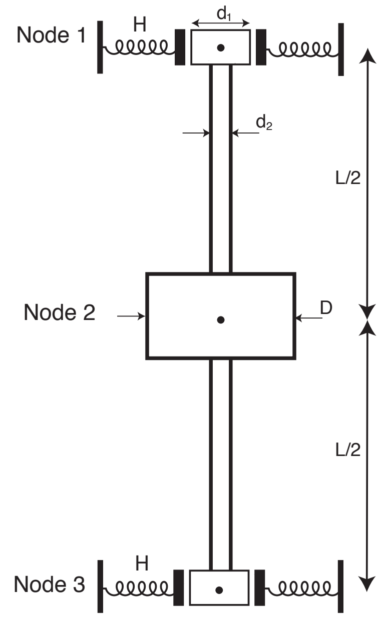

Figure 2. Rotor model

$$K_{ij} = \frac{K_{ij}^{\text{LOP}} + K_{ij}^{\text{LBP}}}{2} + \frac{K_{ij}^{\text{LOP}} - K_{ij}^{\text{LBP}}}{2} cos(4\alpha) \quad (1)$$

$$C_{ij} = \frac{C_{ij}^{\text{LOP}} + C_{ij}^{\text{LBP}}}{2} + \frac{C_{ij}^{\text{LOP}} - C_{ij}^{\text{LBP}}}{2} cos(4\alpha) \quad (2)$$

where $i, j = \xi, \eta$

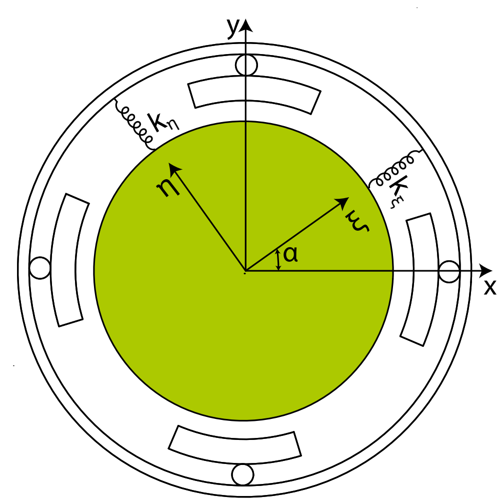

Figure 3. 4−pad bearing geometry, with coordinate system (ξ,η) rotated α degree's from the fixed coordinate system (x, y).

Table 1. The test rig rotor and bearing properties.

Rotor	Symbol	Item	Value	Unit
	d_1	Shaft diameter	49.84	[mm]
	d_2	Shaft diameter	20.00	[mm]
	D	Disc diameter	168	[mm]
	e_m	Mass unbalance radius	70	[mm]
	H	Bearing bracket stiffness	500	[MN/m]
	L	Shaft length	500	[mm]
Bearing	Symbol	Item	Value	Unit
	d	Shaft diameter	49.84	[mm]
	d_b	Bearing diameter	50.09	[mm]
	d_p	Pad diameter	50.15	[mm]
	θ	Pad angle	72	[deg]
	N	No. of pads	4	[-]
	C_b	Diametrical bearing clearance	0.25	[mm]
	C_p	Diametrical pad clearance	0.31	[mm]
	m	Preload factor	0.19	[-]
	x	Pad pivot offset	0.6	[-]

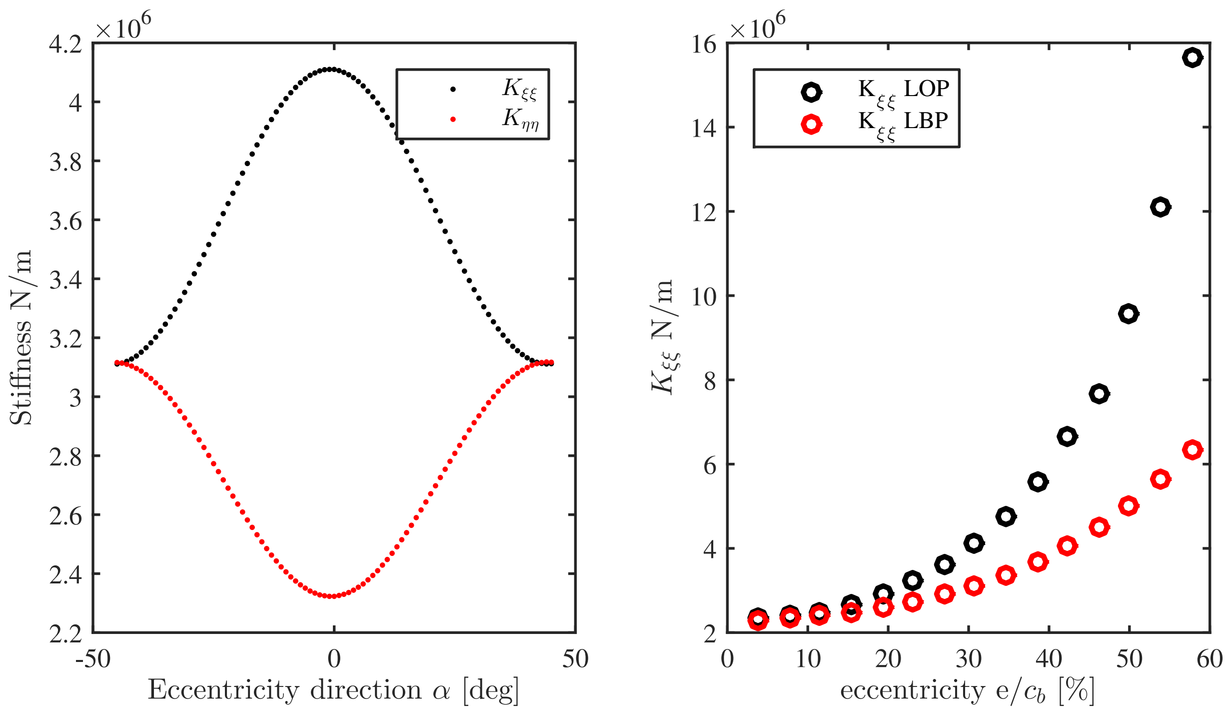

Figure 4. Stiffness as function of α at 30% eccentricity in the coordinate system (ξ,η) (left) and stiffness LOP and LBP as function of eccentricity (right).

The bearing coefficients calculated is in the local coordinate system (ξ,η) and must be transformed using the following transformation [7].

$$\mathbf{K_T} = \mathbf{T}^T \mathbf{K_B} \mathbf{T} \tag{3}$$

$$\mathbf{C_T} = \mathbf{T}^T \mathbf{C_B} \mathbf{T} \tag{4}$$

where

$$\mathbf{T} = \begin{bmatrix} cos(\alpha) & sin(\alpha) \\ -sin(\alpha) & cos(\alpha) \end{bmatrix} \tag{5}$$

and $\mathbf{K_B}$ and $\mathbf{C_B}$ is the bearing stiffness and damping matrices in the local coordinate system (ξ,η).

1.3 Numerical model

Simulations of a vertical rotor with TPJB's are performed with a rotating load

$$f(t) = F_0 * cos(\Omega * t) + F_0 * sin(\Omega * t) \tag{6}$$

applied at the mass position. Here different Ω is studied to see if resonance can occur when 3Ω and 5Ω equals the first natural frequency due to the periodic coefficients in the bearing. The rotor is modelled using Timoshenko beam elements with consistent mass matrix and the bearing coefficients are evaluated at each time-step as function of eccentricity and load angle according to [5]. The equation of motion can thus be written in matrix form as:

$$\mathbf{M}\ddot{u} + (\mathbf{C} + \mathbf{C_T} + \Omega\mathbf{G})\dot{u} + (\mathbf{K} + \mathbf{K_T})u = f(t) \tag{7}$$

where $\mathbf{M}$ is the mass matrix, $\mathbf{C}$ is the damping matrix, $\mathbf{G}$ is the gyroscopic matrix, $\mathbf{K}$ is the stiffness matrix, $\mathbf{K_T}$ and $\mathbf{C_T}$ is the bearing coefficients and Ω is the rotational speed.

From these simulations, displacements can be compared for different rotating speeds Ω to see if resonance peaks can occur for other frequencies than the natural frequencies.

1.4 Numerical simulation

If the bearing coefficients are assumed constant, the Campbell diagram for this system can be calculated. In figure 5 the Campbell diagram is presented and the dashed black lines represent $\Omega, 3\Omega, 5\Omega$. Since the 4-pad bearing setup shows frequency components at 3Ω then the region where $3\Omega = \omega_n$ is of interest to study, where ω_n is the natural frequencies of the system. From the fft diagram in figure 1 there is also a component around 5Ω therefore frequency ranges from 250 rpm to 500 rpm is studied to see if the first mode of vibration could be excited due to the bearing dynamics. Since the bearing coefficients are dependent on the load, two different load cases are considered. For large loads the difference between LOP and LBP is increased and the periodic excitation is increased. Therefore a large force F_0 = 90N and a smaller force F_0 = 23N is evaluated to investigate if load magnitude influence the behaviour of the system.

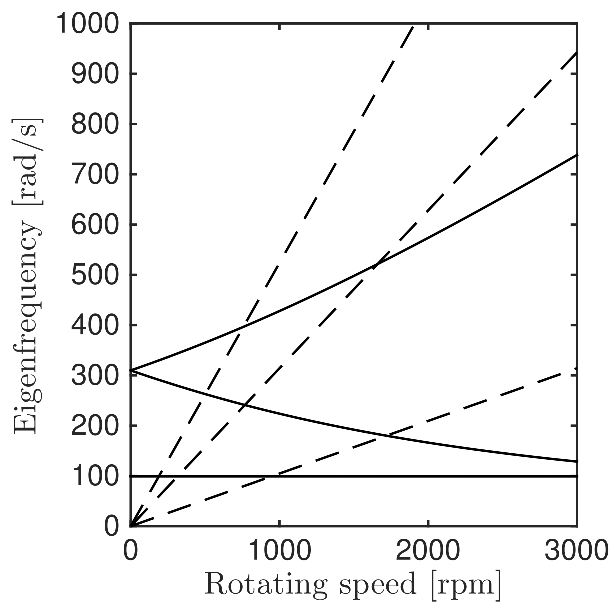

Figure 5. Campbell diagram for constant stiffness at 30% eccentricity assuming LOP.

2. RESULTS AND DISCUSSION

In the numerical simulations the operating speed Ω was set in the range (250 − 500) rpm corresponding to $\Omega/\omega_n = (0.18 - 0.38)$. For each rotating speed 100 periods was recorded and from the last 20 periods the maximum absolute response was calculated for all nodes. Also the maximum and minimum whirl ratio was calculated according to equation 8.

$$\dot{\Theta} = \frac{\dot{y} * x - \dot{x} * y}{(x^2 + y^2) * \Omega} \quad (8)$$

Where the rotational speed Ω is in rad/s. In Figure 6 displacement in the bearing is presented and it can be seen that something changes at $\Omega/\omega_n = 0.2$ and $\Omega/\omega_n = 0.33$.

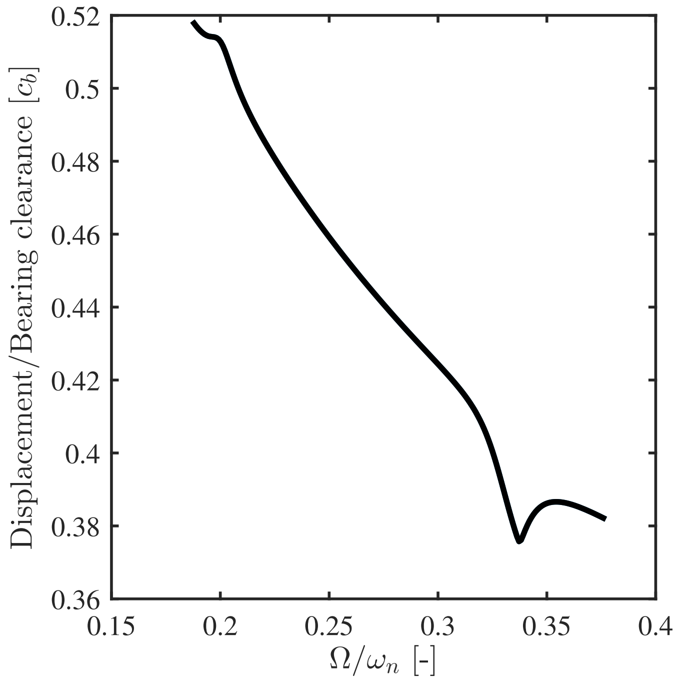

Figure 6. Displacement in the bearing for F_0 = 90 N.

This becomes more clear if studying the disc displacement in Figure 7, here resonance peaks are clearly visible at these frequency multiples. Recall from Figure 4, here it can be seen that the difference between LOP and LBP is large at eccentricities around 45% of the bearing clearance. According to Figure 6 the displacement in the bearing is around 50% of the bearing clearance at $\Omega/\omega_n = 0.2$ and 40% at $\Omega/\omega_n = 0.33$. Since the difference between LOP and LBP is large in this region the frequency component at 3Ω and 5Ω is large and will excite the system.

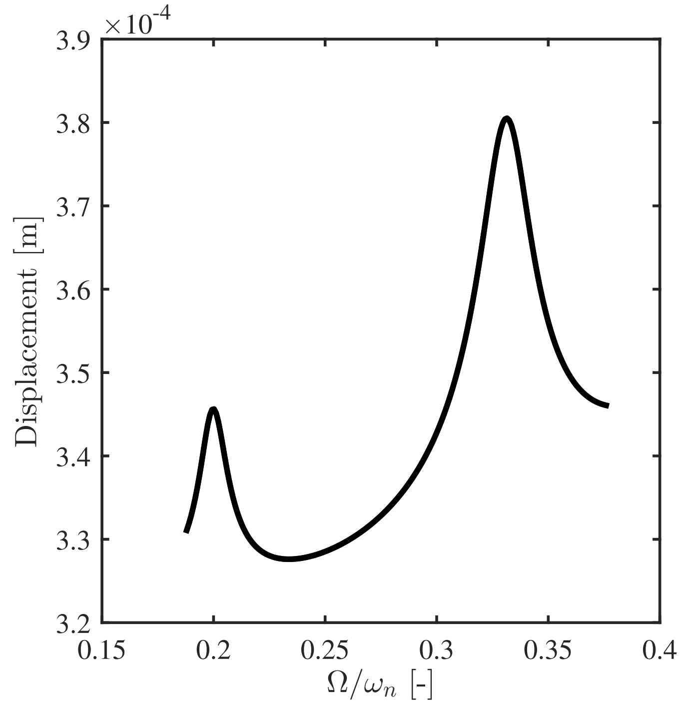

Figure 7. Displacement at the disc for F_0 = 90 N.

In Figure 8 the whirl ratio at the disc is shown, here the maximum and minimum whirl ratio is presented. As seen in Figure 8 the whirl interval is increased especially at the frequency ratio $\Omega/\omega_n = 0.33$. This indicates some other type of dynamic behaviour of the system. In Figure 9 the displacement orbit at rotating speed 440 rpm is presented, this operating speed corresponds to $\Omega/\omega_n = 0.33$ and it shows how the 4-pad bearing effect the dynamics. For low bearing loads the difference between LOP and LBP is small and the periodic behaviour in the bearing is low. This should decrease the periodic excitation and remove the resonance peaks observed in Figure 7.

According to Figure 10 the displacement in the bearing is around 20% of the bearing clearance at $\Omega/\omega_n = 0.2$ and 15% at $\Omega/\omega_n = 0.33$. Recall from Figure 4, here it can be seen that the difference between LOP and LBP is small at eccentricities smaller then 20% of the bearing clearance. Hence the excitation due to the periodic coefficients is small. Comparing the results from the disc displacement in Figure 7 to the disc displacement in Figure 11 the vibration peaks at $\Omega/\omega_n = 0.2$ and $\Omega/\omega_n = 0.33$ has been reduced significantly. From Figure 13 it is clear that the orbit for the smaller load is more circular then for the case of higher load. Also, the whirl ratio interval in Figure 12 is reduced to almost synchronous whirl. The difference between high and low forces is also presented in Figure 14, where the FFT of the disc displacement is presented for the different forces for the operating speed $\Omega = 440$ rpm. Since the periodic excitation is small for low forces the frequency component at 3Ω is negligible and does not excite the first eigenfrequency. However for the large force the frequency component at 3Ω is large and has shown to influence the dynamic response of the machine.

In hydropower machines the number of pads are usually larger then five hence, the periodic stiffness is smaller but with higher frequency. This should decrease the excitation of the machine due to the bearing, but for high bearing loads this can still cause increased vibrations. Most monitoring of the machines are usually in the bearings where displacement and force normally is measured. From these simulations it can be seen that when vibrations occur at the disc position there is a local minimum in the bearing displacement.

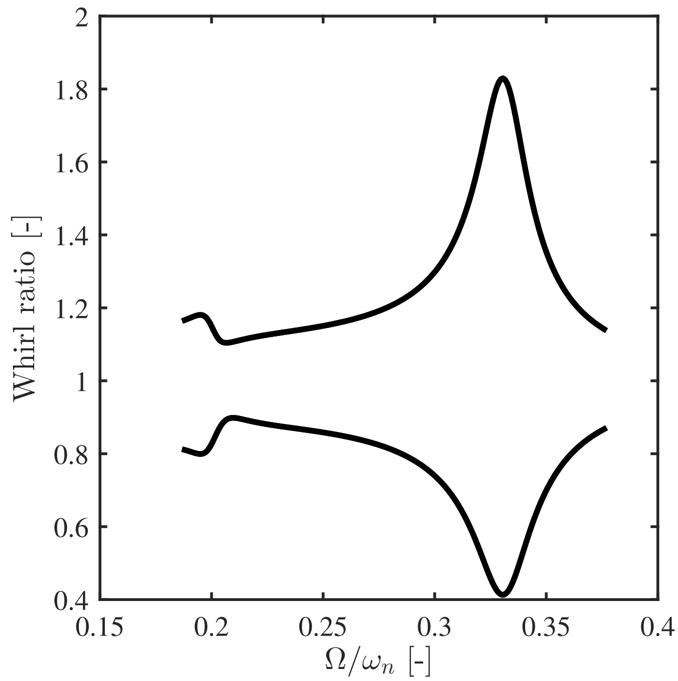

Figure 8. Maximum and minimum whirl ratio at the disc for $F_0 = 90$ N.

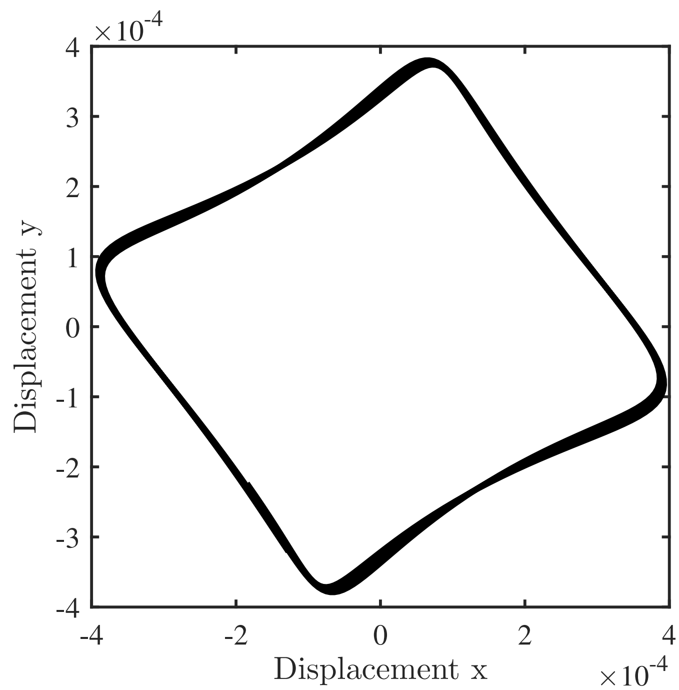

Figure 9. Displacement orbit at the disc for $F_0 = 90$ N

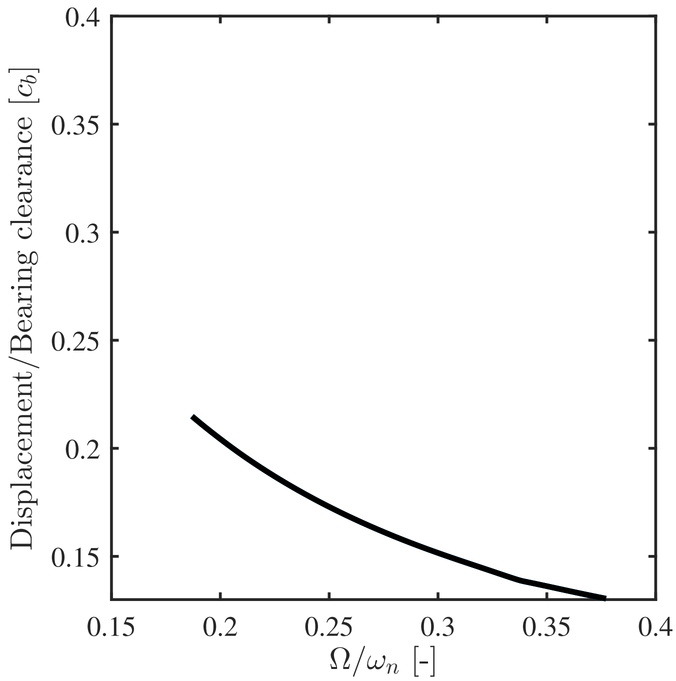

Figure 10. Displacement in the bearing for $F_0 = 23$ N.

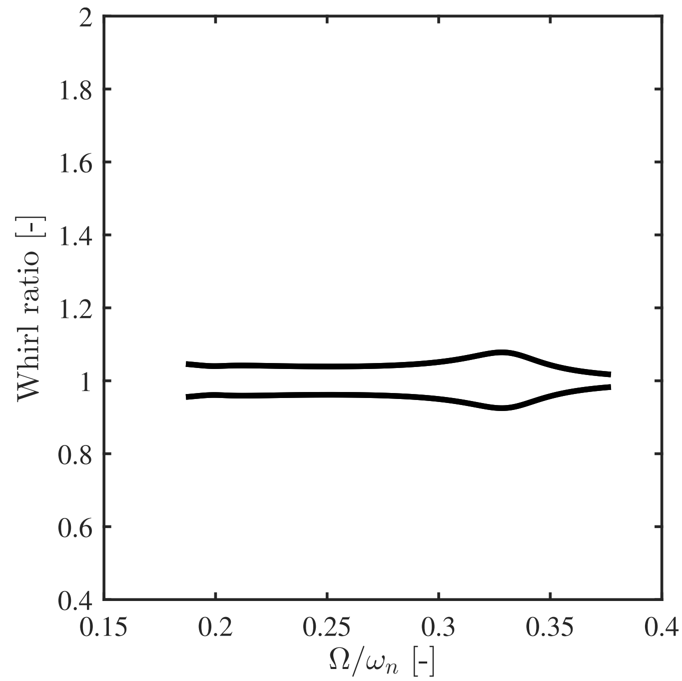

Figure 12. Maximum and minimum whirl ratio at the disc for $F_0 = 23$ N.

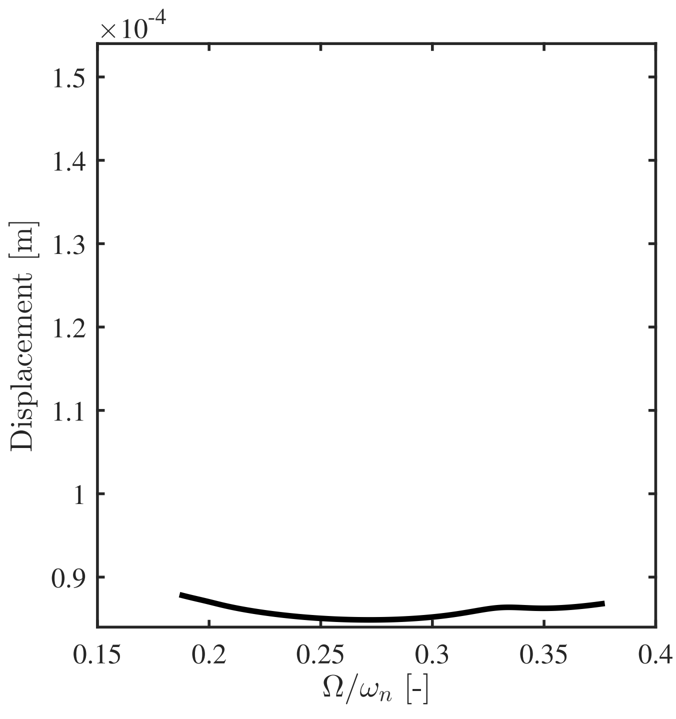

Figure 11. Displacement at the disc for $F_0 = 23$ N

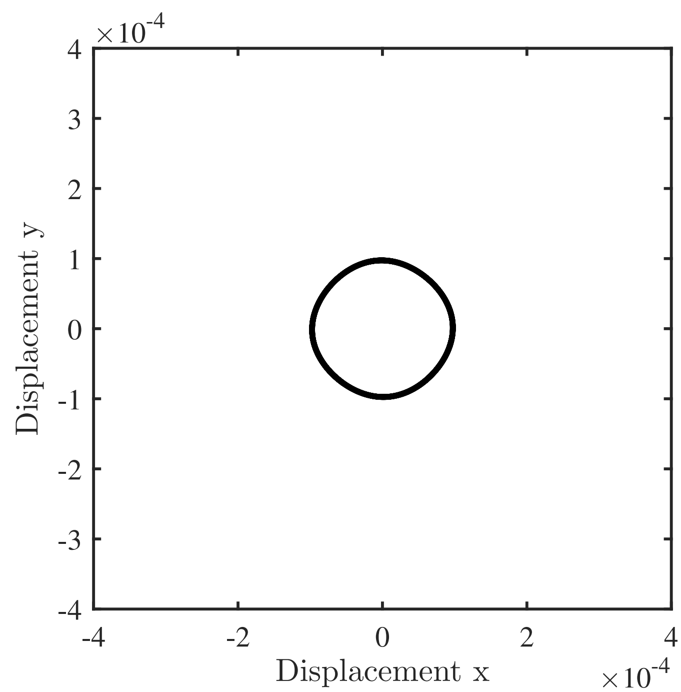

Figure 13. Displacement orbit for the disc where $F_0 = 23$ N

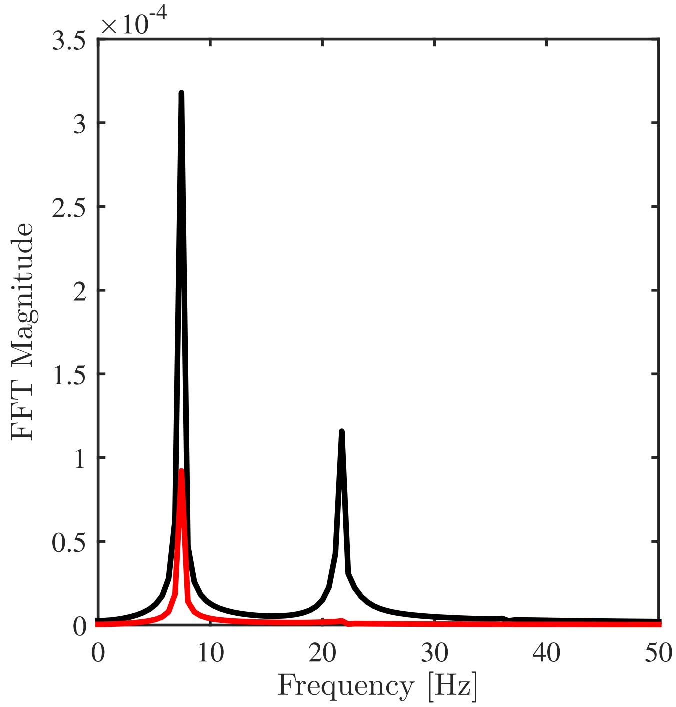

Figure 14. FFT at Ω = 440 rpm where F_0 = 90 N (black) and F_0 = 23 N (red).

3. CONCLUSIONS

In a vertical machine with tilting pad bearings the bearing coefficients will change periodically due to the difference between load on pad and load between pad for a fixed load. In comparison with a horizontal machine the operating point is strongly influenced by the dead weight, hence the bearing coefficients are relatively constant for a fixed load. This paper shows that periodic excitations from the bearing can result in increased vibrations at certain frequencies. The magnitude of the increased vibrations is strongly influenced by the initial load on the system, since the bearing coefficients are increased for higher loads the difference between load on pad and load between pad will increase and this amplifies the periodic excitation. Hence for small loads in the bearing there is almost no periodic excitation and the response is almost unaffected. Interesting is the displacement in the bearing at Ω/ω_n = 0.33 for high loads, the displacement is actually decreased while the displacement at the mass is increased. Since most machines usually are monitored in the bearings the increased vibrations at the disc could be missed. The shaft used for simulations in this paper has been ordered and experiments are planned to verify if the bearings dynamics can excite the system.

ACKNOWLEDGMENTS

The research presented was carried out as a part of "Swedish Hydropower Centre - SVC". SVC has been established by the Swedish Energy Agency, Elforsk and Svenska Kraftnät together with Luleå University of Technology, The Royal Institute of Technology, Chalmers University of Technology and Uppsala University. www.svc.nu.

REFERENCES

[1] JW Lund. Spring and damping coefficients for the tilting-pad journal bearing. *ASLE transactions*, 7(4):342–352, 1964.

[2] Timothy Dimond, Amir Younan, and Paul Allaire. A review of tilting pad bearing theory. *International Journal of Rotating Machinery*, Vol. 2011(No. 908469), 2011.

[3] Matthew Cha and Sergei Glavatskih. Nonlinear dynamic behaviour of vertical and horizontal rotors in compliant liner tilting pad journal bearings: Some design considerations. *Tribology International*, 82, Part A(0):142 – 152, 2015.

[4] Maurice F White, Erik Torbergsen, and Victor A Lumpkin. Rotordynamic analysis of a vertical pump with tilting-pad journal bearings. *Wear*, 207(1–2):128 – 136, 1997.

[5] Mattias Nässelqvist, Rolf Gustavsson, and Jan-Olov Aidanpää. Experimental and numerical simulation of unbalance response in vertical test rig with tilting-pad bearings. *International Journal of Rotating Machinery*, Vol. 2014(No. 309767), 2014.

[6] Rotordynamic-Seal Research.

[7] R. D. Cook. *Concepts and applications of finite element analysis*. Wiley, S.l, 1989.